38th Fluid Dynamics Conference and Exhibit
23 - 26 June 2008, Seattle, Washington

AIAA 2008-3854

Hybrid RANS-LES Turbulence Models on Unstructured Grids

C. Eric Lynch* and Marilyn J. Smith†

School of Aerospace Engineering, Georgia Institute of Technology, Atlanta, Georgia, 30332-0150, USA

This work evaluates the ability of a hybrid Reynolds-Averaged Navier-Stokes (RANS) and Large Eddy Simulation (LES) turbulence method to accurately predict the physics of an unsteady separated flow field in an unstructured legacy RANS computational fluid dynamics code. The hybrid method consists of a blending of the $k-\omega$ SST RANS model with a one-equation LES model for the subgrid-scale turbulent kinetic energy (k^{sgs}). Unstructured grids provide better resolution of complex geometries which is the motivation for extending this method. Correlations include theoretical data, experimental data and computational results with RANS turbulence models.

Nomenclature

e	Specific internal energy
E	Total energy
h	Specific enthalpy
i, j, k	Unit vectors in the x,y,z directions
k	Turbulent kinetic energy
l	Length
M	Mach number
n	Number of rotor blades
Pr_L	Laminar Prandtl number, $Pr_L = \frac{c_p \mu}{\kappa}$
q	Heat flux vector
t	Time
T	Temperature
u, v, w	Velocity in the x, y, z directions
x, y, z	Cartesian coordinate system in the stream, normal and span directions
y^+	Dimensionless sublayer-scaled distance, $u_T y/\nu$
V	Velocity
δ_{ij}	Kronecker delta, when i=j, $\delta_{ii} = 1$, otherwise, $\delta_{ij} = 0$
Δ	Local grid cell size
ϵ	Dissipation per unit mass
η	Kolmogorov length scale
κ	Thermal conductivity
μ	Molecular viscosity or advance ratio
μ_T	Eddy viscosity
ν	Kinematic molecular viscosity, μ/ρ
ρ	Mass density
σ_{ij}	Instantaneous viscous stress tensor

*Ph.D. Student, Graduate Research Assistant and AIAA Student Member.
†Associate Professor and AIAA Associate Fellow.

τ_{ij} Reynolds shear stress tensor
ω Vorticity

Subscripts and Superscripts
i, j, k Tensor directions
k Kinetic energy
l Length
L Laminar
sgs Subgrid-scale
T Turbulent
$(.)'$ Fluctuating term for a time-averaged quantity
$(.)''$ Fluctuating term for a Favre-averaged quantity
$\vec{(.)}$ Vector quantity
$\overline{(.)}$ Mean quantity
$\widetilde{(.)}$ Mass-averaged quantity
∞ Free stream

I. Introduction

While computational fluid dynamics (CFD) is considered by some to be a mature technology, there still remain gaps in the numerical closure of the Navier-Stokes equations, known as turbulence modeling. Indeed the argument can be made that while major advances in computational hardware have occurred in the past two decades, the ability to efficiently (in an engineering sense) capture complex flow field turbulent structures has lagged the advances made in other areas. While the much more computationally intensive Large Eddy Simulations (LES) and Direct Numerical Simulations (DNS) are performed in research environments, simulations that resolve the Reynolds-Averaged Navier-Stokes (RANS) equations are still required for rapid engineering results. In the past decade, some strides have been made in bridging this gap by the development of hybrid turbulence techniques that combine RANS and LES methods to address applications with strong separated flow fields.

There are many existing RANS turbulence models,[1] including algebraic (Baldwin-Lomax), one-equation (Baldwin-Barth, Spalart-Allmaras), and two-equation ($k-\omega$, $k-\omega$ SST) models. For applications of even simple aerodynamic configurations such as airfoils and wings,it is clear [2,3] that these RANS models are failing when the flow field becomes highly unsteady with viscous-dominated features such as in static or dynamic stall. Since RANS models are statistical approximations of the turbulence at all length scales (figure 1), and are tuned using a small subset of test cases, most of which have a flow field that is steady and attached, these problems are not surprising.

For separated flows, either LES or DNS is needed so that at a minimum the large turbulence scales can be captured rather than statistically modeled. Large Eddy Simulations (LES) mass-average the compressible governing equations, followed by a filtering process wherein turbulence eddies that are larger than the grid size are captured and turbulence with scales smaller than the grid is modeled. DNS is a process by which turbulence scales are captured directly, requiring an extremely large grid and extensive computational resources. While LES is capable of capturing the larger eddies using grids that are much coarser than those needed for DNS, the small time step sizes and grid constraints near configuration surfaces at moderate to high Reynolds numbers still keeps it beyond the scope of many engineering needs.

Research into hybrid turbulence techniques is a topic of interest as a means to close the gap between RANS and LES. This has been demonstrated by Sanchez-Rocha *et al.*[5] who incorporated the $k-\omega SST$ RANS model into an existing LES code as a mechanism to moderate the excessively high cost to resolve the turbulent eddies near the wall. He has demonstrated this on a NACA0015 airfoil at a Reynolds number of 1 million. Another approach has been to resolve the subgrid scale models of turbulence within an existing RANS code, utilizing an existing RANS model where separation effects are minimal. Thus even for coarse

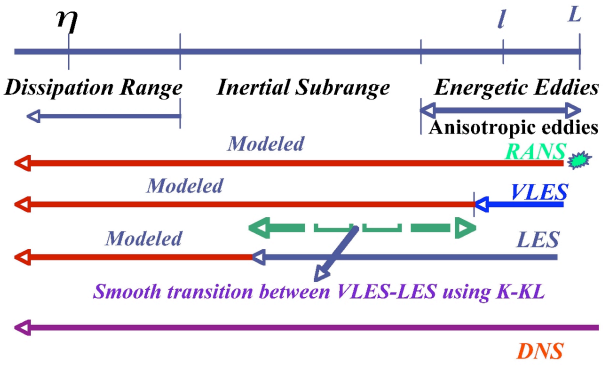

Figure 1. Illustration of the resolution of turbulence scales by numerical techniques.[6]

grids, more suitable for RANS or Very-Large Eddy Simulation (VLES), some enhancement of the physics should be captured. Of these hybrid methods, the most well-known is Detached Eddy Simulation (DES),[4] typically applied in conjunction with the $k-\omega SST$ Menter[7] or Spalart-Allmaras[8] RANS turbulence models.

These two approaches to hybrid RANS-LES are different in the sense of the underlying methodologies. LES codes are typically explicit, with high order spatial and temporal schemes. Care is taken to include most, if not all, of the fluctuating terms that appear when mass (Favre)-averaging the compressible Navier-Stokes equations. Within existing CFD (RANS) codes, the spatial and temporal schemes are usually lower order spatial and temporal schemes. The temporal integration is typically implicit to accelerate the simulation. Fluctuating terms appearing from the time-averaging of usually the incompressible Navier-Stokes equations may have less computationally consuming "shortcuts". Finally, the schemes may be overly dissipative, resulting in a smearing of the features of the flow field.

For this effort, the HRLES hybrid model chosen was developed by Sanchez-Rocha *et al.*,[5] and is based on a two-equation RANS model, blended with an LES resolution of the k-equation, resulting in a modified value of the turbulent eddy viscosity. A second Very Large Eddy Simulation (VLES) technique that resolves the k and $k\ell$ turbulence equations was developed by Fang and Menon.[9,10] Both models were successfully ported to a legacy structured CFD solver (OVERFLOW) and demonstrated[6] for 2D airfoils and the UH-60A rotor. This paper documents the experience in taking the HRLES model and implementing it in a legacy unstructured RANS methodology.

II. Governing Equations of Motion

The instantaneous Navier-Stokes equations for compressible flows can be expressed in tensor form as

$$\frac{\partial \rho}{\partial t} + \frac{\partial}{\partial x_j}(\rho u_j) = 0 \tag{1}$$

$$\frac{\partial}{\partial t}(\rho u_i) + \frac{\partial}{\partial x_j}(\rho u_i u_j) + \frac{\partial p}{\partial x_i} - \frac{\partial \sigma_{ji}}{\partial x_j} = 0$$

$$\frac{\partial}{\partial t}[\rho(e + 0.5 u_i u_i)] + \frac{\partial}{\partial x_j}[\rho u_j (h + 0.5 u_i u_i)] + \frac{\partial q_j}{\partial x_j} - \frac{\partial}{\partial x_j}(u_i \sigma_{ij}) = 0$$

For flows relevant to the standard aerodynamic applications, several assumptions about the flow can be made to affect closure of these equations. The flows of interest are assumed to be in the moderate temperature range (incompressible to supersonic Mach regimes), comprised of a Newtonian fluid consisting of a monotonic gas with isotropic viscosity. Thus the perfect gas law and the Boussinesq constitutive relation can be applied.

The difference between RANS and LES first appears in the averaging technique applied to the Navier-Stokes equations. RANS equations apply Reynolds averaging where the primitive variables $(\rho, \vec{V}, p, e)$ are separated into mean $(\overline{f})$ and fluctuating (f') components, then averaged over a finite period of time much greater than the turbulent fluctuation frequency, so that the mean value of single fluctuating variable will be zero. The mean value of some multiplied fluctuating variables will remain non-zero, and these correlated values must be treated via additional closure assumptions. This Reynolds-averaging process is also typically applied to the incompressible Navier-Stokes equations to obtain closures for the boundary layer. For LES applications, density, heat transfer and pressure remain as Reynolds-averaged values, while the remainder of the pertinent variables are decomposed using a Favre-averaging that accounts for compressibility effects, and yields mass-averaged $(\widetilde{f})$ and fluctuating (f'') components. It should be noted that the fluctuating terms that arise in the Favre and Reynolds averaging processes are not identical and therefore are typically assigned different notations.

The compressible Navier-Stokes equations, once Favre-averaged, can be mathematically formulated as :

$$\begin{aligned}
\frac{\partial \overline{\rho}}{\partial t} + \frac{\partial}{\partial x_j}(\overline{\rho}\widetilde{u_j}) &= 0 \\
\frac{\partial}{\partial t}(\overline{\rho}\widetilde{u_i}) + \frac{\partial}{\partial x_j}(\overline{\rho}\widetilde{u_i}\widetilde{u_j}) &= -\frac{\partial \overline{p}}{\partial x_i} + \frac{\partial \overline{\sigma_{ij}}}{\partial x_j} - \frac{\partial}{\partial x_j}(\overline{\rho u_i'' u_j''}) \\
\frac{\partial}{\partial t}[\overline{\rho}(\widetilde{e} + 0.5\widetilde{u_i}\widetilde{u_i})] + \frac{\partial}{\partial x_j}[\overline{\rho}\widetilde{u_j}(\widetilde{h} + 0.5\widetilde{u_i}\widetilde{u_i})] &= \frac{\partial}{\partial x_j}(-q_{L_j} + \widetilde{u_i}\overline{\sigma_{ij}}) - \frac{\partial}{\partial t}[0.5\overline{\rho u_i'' u_i''}] \\
&\quad + \frac{\partial}{\partial x_j}[-\widetilde{u_j}\overline{\rho u_i'' u_j''} + \widetilde{u_j}0.5\overline{\rho u_i'' u_i''} - \overline{\rho u_j'' h''} \\
&\quad + \overline{\sigma_{ji} u_i''} - 0.5\overline{\rho u_j'' u_i'' u_i''}]
\end{aligned} \tag{2}$$

As a result of the averaging processes for incompressible or compressible assumptions, there arises a Reynolds-stress tensor that requires closure, either in the specific Reynolds-averaged form $(\tau_{ij} = -\overline{u_i' u_i'})$ or the compressible Favre-averaged form $(\overline{\rho}\tau_{ij} = -\overline{\rho u_i'' u_i''})$. The turbulent kinetic energy can then be defined in its specific formulation $k = 0.5\overline{u_i' u_i'}$ or full form $\overline{\rho}k = 0.5\overline{\rho u_i'' u_i''}$, respectively. Favre-averaging also gives rise to the the turbulent heat flux $(q_{Ti} = \overline{\rho u_i'' h''})$ and the rate of turbulent dissipation $(\overline{\rho}\epsilon = \overline{\sigma_{ji}\frac{\partial u_i''}{\partial x_j}})$. For flows up through the low supersonic regime, the molecular diffusion and turbulent transport terms $(\overline{\sigma_{ji} u_i''} - \overline{\rho u_j'' 0.5 u_i'' u_i''})$ are typically ignored,[1] and this practice is continued for this analysis. The additional equations through which these terms are resolved or closed gives rise to the turbulence model of the simulation.

$$\begin{aligned}
\frac{\partial \overline{\rho}}{\partial t} + \frac{\partial}{\partial x_j}(\overline{\rho}\widetilde{u_j}) &= 0 \\
\frac{\partial}{\partial t}(\overline{\rho}\widetilde{u_i}) + \frac{\partial}{\partial x_j}(\overline{\rho}\widetilde{u_i}\widetilde{u_j}) &= -\frac{\partial \overline{p}}{\partial x_i} + \frac{\partial \overline{\sigma_{ij}}}{\partial x_j} - \frac{\partial}{\partial x_j}(\overline{\rho}\tau_{ij}) \\
\frac{\partial}{\partial t}[\overline{\rho}(\widetilde{e} + 0.5\widetilde{u_i}\widetilde{u_i})] + \frac{\partial}{\partial x_j}[\overline{\rho}\widetilde{u_j}(\widetilde{h} + 0.5\widetilde{u_i}\widetilde{u_i})] &= \frac{\partial}{\partial x_j}(-q_{L_j} + \widetilde{u_i}\overline{\sigma_{ij}}) - \frac{\partial}{\partial t}[\overline{\rho}k] \\
&\quad + \frac{\partial}{\partial x_j}[-\widetilde{u_j}\overline{\rho}\tau_{ij} + \widetilde{u_j}\overline{\rho}k - q_{T_j}]
\end{aligned} \tag{3}$$

If symmetry is assumed, the Reynolds-stress tensor yields six unknowns that are approximated using models about the behavior of the fluctuating correlations, $\overline{u_i'' u_j''}$. These approximations yield the set of RANS turbulence models, ranging from algebraic to two-equation techniques. It was previously noted that the current practice is to assume the Boussinesq approximation, which can be utilized to relate the fluctuations to an eddy viscosity, μ_T:

$$\overline{\rho}\tau_{ij} = 2\mu_T[S_{ij} - \frac{1}{3}\frac{\partial \widetilde{u_k}}{\partial x_k}\delta_{ij}] - \frac{2}{3}\overline{\rho}k\delta_{ij} \tag{4}$$

Similarly, the turbulent heat flux vector can be related to the eddy viscosity, μ_T, via proportionality to the mean temperature gradient:

$$q_{Ti} = -\frac{\mu_T}{Pr_T}\frac{\partial \widetilde{h}}{\partial \widetilde{x_j}} = -\frac{\mu_T c_p}{Pr_T}\frac{\partial \widetilde{T}}{\partial \widetilde{x_j}} \tag{5}$$

that introduces the turbulent Prandtl number, Pr_T, which can be either constant or variable, depending on the application. Finally, the rate of turbulent dissipation can be expressed as

$$\overline{\rho}\epsilon = \overline{\mu[2S_{ji}S''_{ij} - \frac{2}{3}u_{kk}u''_{ii}]} \tag{6}$$

In addition to the Favre-averaging, the concept of LES is based on the direct capture of the large turbulence eddies as part of the solution of the Favre-averaged Navier-Stokes equations, relegating the smaller turbulent eddies to be modeled. This process is based on the view that the larger turbulence eddies contribute significantly to the Reynolds-stress tensor, while the smaller eddies are less significant. In order to separate these effects, in addition to the averaging process, the variables in the equation of motion should also be filtered (typically referred to as Favre-filtering) to obtain the small or subgrid scale (sgs) turbulence. These filtering techniques are discussed in Wilcox.[1] Near the surface of the configuration undergoing simulation, the turbulence eddy scales reduce significantly, requiring in LES a very refined grid that increases the computational resources beyond the reach of most engineering applications. As attached boundary layer characteristics can be well-predicted by RANS turbulence models, an alternative to grid refinement is to switch the simulation between RANS and LES.

III. Hybrid RANS-LES Model

The correlation of these turbulence terms requiring closure to viscosity permits the RANS and LES turbulence approximations to be combined to provide closure information in the simulation. The information exchange occurs via the turbulent kinetic energy, k. In this work, the RANS turbulence model chosen to effect this closure is the Menter $k\omega - SST$ turbulence model,[7] based on its success in prior CFD applications of interest to the authors.[6,12,13]

The Menter $k\omega - SST$ turbulence model resolves two differential equations that describe the turbulent kinetic energy, k, as well as an approximation for the length scale based on the dissipation per unit turbulent kinetic energy, ω. These equations are given by:

$$\frac{\partial}{\partial t}(\rho k) + \frac{\partial}{\partial x_j}(\rho u_j k) = \tau_{ij}^{rans}\frac{\partial u_i}{\partial x_j} - \beta^*\rho\omega k + \frac{\partial}{\partial x_j}\left[(\mu + \sigma_k\mu_T)\frac{\partial k}{\partial x_j}\right] \tag{7}$$

$$\frac{\partial}{\partial t}(\rho\omega) + \frac{\partial}{\partial x_j}(\rho u_j \omega) = \frac{\gamma\rho}{\mu_T}\tau_{ij}^{rans}\frac{\partial u_i}{\partial x_j} - \beta\rho\omega^2 + \frac{\partial}{\partial x_j}\left[(\mu + \sigma_\omega\mu_T)\frac{\partial \omega}{\partial x_j}\right] + 2(1-F_2)\rho\sigma_{\omega 2}\frac{1}{\omega}\frac{\partial k}{\partial x_j}\frac{\partial \omega}{\partial x_j} \tag{8}$$

where the *rans* superscript is used to denote the use of the Reynolds-averaged Reynolds-stress tensor. Menter[7] indicates that the production terms ($\tau_{ij}^{rans}\frac{\partial u_i}{\partial x_j}$) can be modeled directly with $\mu_T\Omega^2$ where Ω is the vorticity magnitude defined by $\Omega^2 = (w_y - v_z)^2 + (u_z - w_x)^2 + (v_x - u_y)^2$.

The LES turbulent kinetic energy equation to obtain the subgrid scale data is one successfully used by Kim and Menon[14] :

$$\frac{\partial}{\partial t}(\overline{\rho}k^{sgs}) + \frac{\partial}{\partial x_j}(\overline{\rho}\widetilde{u_j}k^{sgs}) = \tau_{ij}^{sgs}\frac{\partial \widetilde{u_i}}{\partial x_j} - C_\epsilon\overline{\rho}\frac{(k^{sgs})^{3/2}}{\Delta} + \frac{\partial}{\partial x_j}\left[\left(\frac{\widetilde{\mu}}{Pr} + \frac{\mu_{sgs}}{Pr_t}\right)\frac{\partial k^{sgs}}{\partial x_j}\right] \tag{9}$$

Baurle *et al.*[15] have demonstrated that RANS and LES methods can be linearly merged to form a hybrid model. Speziale[16] proposed an extension to this via the Reynolds-stress tensor. Thus the RANS equations of motion and kinetic energy equation would be recast in the generic form:

$$\frac{\partial}{\partial t}(\vec{F}) + \frac{\partial}{\partial x_j}(\widetilde{u_j}\vec{F}) = \frac{\partial}{\partial x_j}(\vec{G}^{trans}) + \vec{G}^{src} + \frac{\partial}{\partial x_j}(\vec{G}^{hybrid}_{T_{trans}}) + \vec{G}^{hybrid}_{T_{src}} \tag{10}$$

where $\vec{E} = \{\rho, \rho\widetilde{u_j}, \rho E, \rho k\}$ and the right hand side of the equation consists of the original transport ($\vec{G}^{trans}$) and source ($\vec{G}^{src}$) vectors excluding the fluctuating turbulence terms, which have been formulated into new vectors, $\vec{G}_{T_{trans}}$ and $\vec{G}_{T_{src}}$ that will be hybridized. The hybridization of the two $\vec{G}_T$ terms occurs via a simple linear formulation $\vec{G}^{hybrid}_T = F\vec{G}^{rans}_T + (1-F)\vec{G}^{sgs}_T$. The function F which is used as the switch mechanism is $F = tanh(x^4)$ where $x = max(\frac{2\sqrt{k}}{0.09\omega y}, \frac{500\nu}{y^2\omega})$.

Further details of the development of this hybridization technique can be found in Sanchez-Rocha and Menon.[5]

IV. Computational Methodology

The hybrid RANS/LES model has been extended for unstructured topologies and implemented into NASA Langley's unstructured CFD solver FUN3D. FUN3D implicitly solves the Reynolds Averaged Navier-Stokes (RANS) equations using node-centered unstructured mixed topological meshes[11,17,18] and has been successfully utilized for a number of applications that encompass the aerospace spectrum.[19–21] FUN3D can resolve the RANS equations for both compressible and incompressible[22] Mach regimes. Steady state solutions are obtained using a first-order backward Euler scheme with local time stepping, while time accurate solutions utilize the second-order backward differentiation formula (BDF). The resulting linear system of equations is solved using a point-implicit relaxation scheme. Turbulence models include the Spalart-Allmaras[8] and Menter $k\omega - SST$[7] models, in addition to the modifications accomplished as part of this paper. The Roe flux difference splitting technique[23] is utilized to calculate the inviscid fluxes on the control volume faces, while viscous fluxes are computed using a finite volume formulation that results in an equivalent central difference approximation.

When implementing the HRLES scheme, it is necessary to recognize that the computational scheme is typically nondimensionalized. Thus, the equations delineated in the prior sections must be modified to work within the existing scheme. For FUN3D, the nondimensionalization consists of the following:

$$\rho = \frac{\tilde{\rho}}{\tilde{\rho}_\infty}, \quad u_j = \frac{\tilde{u}_j}{\tilde{a}_\infty}, \quad k = \frac{\tilde{k}}{\tilde{a}^2_\infty}, \quad \omega = \frac{\tilde{\mu}_\infty\tilde{\omega}}{\tilde{\rho}_\infty\tilde{a}^2_\infty}$$

$$x_j = \frac{\tilde{x}_j}{\tilde{L}} \Longrightarrow \frac{\partial}{\partial\tilde{x}_j} = \frac{\partial}{\partial x_j}\frac{\partial x_j}{\partial\tilde{x}_j} = \frac{1}{\tilde{L}}\frac{\partial}{\partial x}$$

$$t = \frac{\tilde{t}}{\tilde{L}/\tilde{a}_\infty} \Longrightarrow \frac{\partial}{\partial\tilde{t}} = \frac{\partial}{\partial t}\frac{\partial t}{\partial\tilde{t}} = \frac{\tilde{a}_\infty}{\tilde{L}}\frac{\partial}{\partial t}$$

where the tilde represents a dimensional variable. The effect of this nondimensionalization is illustrated here with the k and ω turbulence equations:

$$\frac{\partial}{\partial t}(\rho k^{rans}) + \frac{\partial}{\partial x_j}(\rho u_j k^{rans}) = \frac{M_\infty}{Re}\frac{\mu_T}{\rho}\Omega^2 - \frac{Re}{M_\infty}\beta^*\rho\omega k^{rans} + \frac{\partial}{\partial x_j}\left[(\mu + \sigma_k\mu_T)\frac{\partial k}{\partial x_j}\right] \tag{11}$$

$$\frac{\partial}{\partial t}(\rho k^{sgs}) + \frac{\partial}{\partial x_j}(\rho u_j k^{sgs}) =$$

$$\frac{M_\infty}{Re}\frac{\mu_T}{\overline{\rho}}\left[2u_x^2 + u_y^2 + u_z^2 + v_x^2 + 2v_y^2 + v_z^2 + w_x^2 + w_y^2 + 2w_z^2 + 2u_yv_x + 2u_zw_x + 2v_zw_y\right]$$

$$-\frac{2}{3}\frac{M_\infty}{Re}\frac{\mu_T}{\overline{\rho}}\left(u_x + v_y + w_z\right)^2 - \frac{2}{3}k^{sgs}\left(u_x + v_y + w_z\right)$$

$$+C_\epsilon\rho\frac{k^{sgs\,3/2}}{\Delta} + \frac{\partial}{\partial x_j}\left[\left(\frac{\mu}{Pr} + \frac{\mu^{sgs}}{Pr_t}\right)\frac{\partial k^{sgs}}{\partial x_j}\right] \tag{12}$$

$$\frac{\partial}{\partial t}(\rho\omega)+\frac{\partial}{\partial x_j}(\rho u_j\omega)=\frac{M_\infty}{Re}\gamma\rho\Omega^2-\frac{Re}{M_\infty}\beta\rho\omega^2+2(1-F_2)\frac{Re}{M_\infty}\rho\sigma_{\omega 2}\frac{1}{\omega}\frac{\partial k}{\partial x_j}\frac{\partial \omega}{\partial x_j}+\frac{\partial}{\partial x_j}\left[(\mu+\sigma_\omega\mu_T)\frac{\partial\omega}{\partial x_j}\right] \quad (13)$$

V. Test Cases

V.A. Circular Cylinder

The first test case for this methodology is the flow of air over a circular cylinder at a Mach number of 0.2 and a diameter-based Reynolds number of 3900 at standard sea-level conditions. The two-dimensional case was a structured O-mesh that was converted to form an unstructured hex grid. The structured grid included 200 nodes in the wrap-around direction with 139 points expanding radially outward with a 10% stretching ratio, yielding a $y+ < 0.02$. While the wake was somewhat coarse due to the uniform spacing of the grid as seen in figure 2, it was instrumental in verifying the implementation of the model, allowing a direct comparison with the structured methodology implementations.

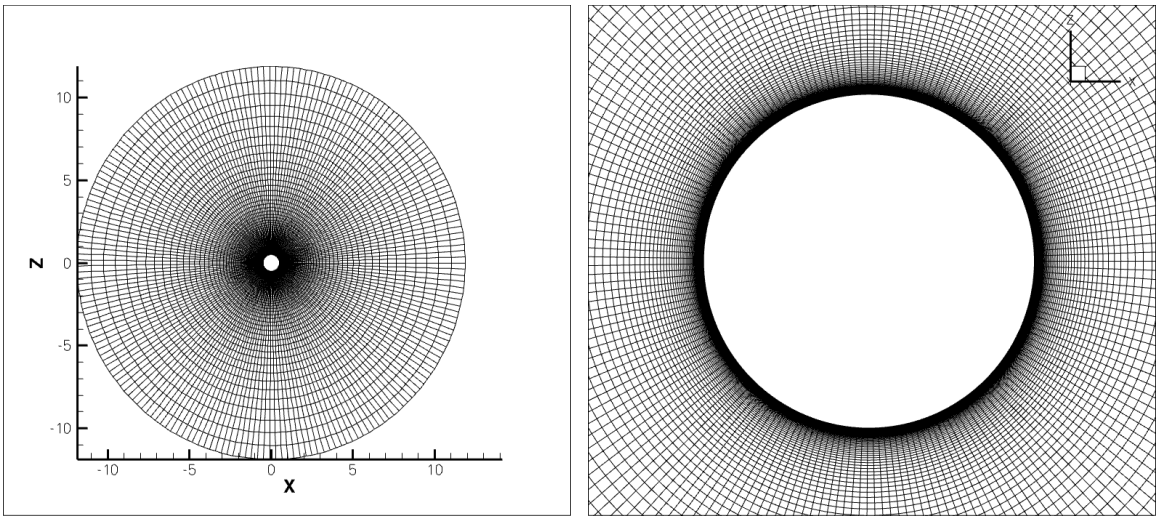

(a) Centerline Cylinder Grid Slice (b) Centerline Cylinder Grid Slice (Close Up)

Figure 2. Computational Grid for the 2D Cylinder

For this test case a nondimensional time step of 0.119 was selected to obtain approximately 200 steps per shedding cycle, assuming Strouhal number of 0.21.

V.B. NACA0015 Airfoil

The NACA 0015 airfoil wing was also selected as an initial test case because of the difficulty that RANS turbulence models have had in capturing the physics of the stalled configuration.[6] Further, there are experimental data[24] with which correlations can be made.

For this configuration, the grid was once again a structured grid that was converted into an unstructured hex grid topology (See figure 3). The grid consisted of 539 points in streamwise direction, with 391 of the grid points located on the wing. There were 97 points in the normal direction, yielding a y+ of less than 1. This was the same grid utilized by Sanchez-Rocha *et al.*[5] and Shelton *et al.*[6] for studies using similar methodologies.

The run conditions were set to a Mach number of 0.291 with a Reynolds number per chord (=1) of 1.955 million. Various angles of attack were simulated in the attached and stalled region. A physical time step of 0.00287 seconds was chosen, which was similar to the time step employed by Shelton *et al.*[6]

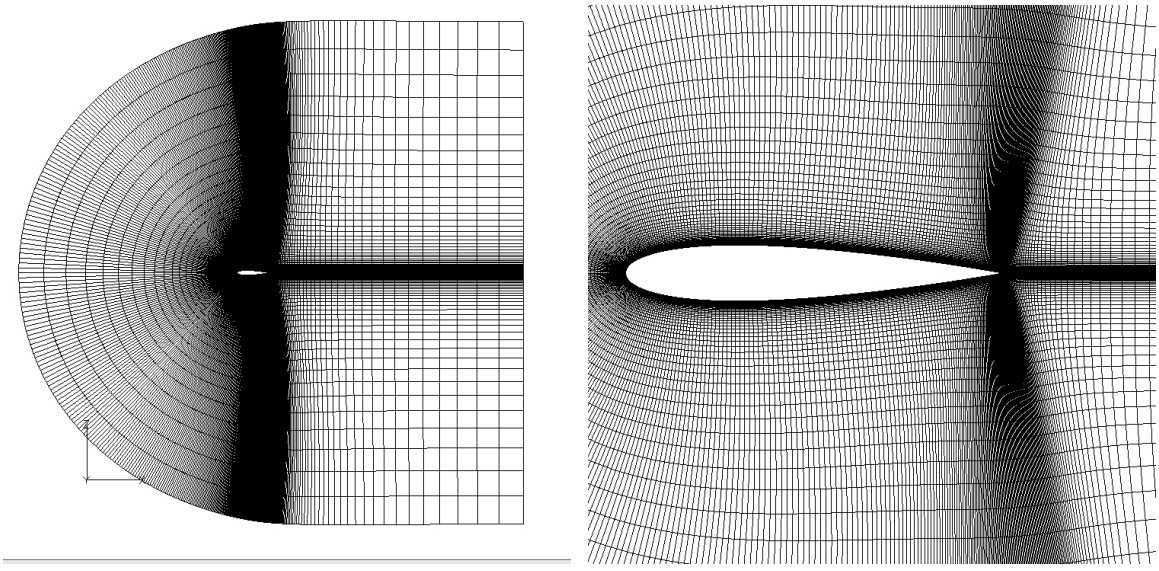

(a) Airfoil Grid (b) Close up of Airfoil Grid

Figure 3. Computational Grid for the NACA0015 Wing

VI. Results

VI.A. Circular Cylinder

Examination of figure 4 shows that HRLES captures the physics associated with the vortex shedding much more accuractely when compared to the baseline $k-\omega SST$ RANS results that have been run on the identical grid and with the same numerical options. The RANS solution shows that the vortex shedding process has been completely smoothed out by the model, while the vortex wake of the HRLES is much more physical. This is born out when the values of the turbulent kinetic energy are observed, as in figure 5, where the turbulent kinetic energy shows a smeared wake region with no periodicity. Figure 6 is a graphical representation of how the two models are blended. Here, values near 0 indicate LES-dominated regions and values near 1 indicate RANS-dominant regions. Near the surface and attached regions, the value of the blending function is close to 1, indicating that the RANS model is in force. In the wake and aft of the separation point, the function is essentially zero showing that the flow field turbulence characteristics are dominated by the LES-computed turbulence.

The instantaneous pressure coefficient on the cylinder is plotted in figure 7 for both the RANS and hybrid model. Both simulations show a shift slightly forward of the minimum pressure location from experiment,[26] but the magnitude of the HRLES simulation is within 3% of the experimental magnitude, while the RANS model is about 18% in error of the value.

The computed Strouhal number for the HRLES run is 0.25, compared with the experimental[25] value of 0.215 ± 0.005. The RANS simulation did not shed vorticity, thus it was not possible to compute a Strouhal number. The separation point predicted by the HRLES method is 86.5^o, while the RANS method predicts separation at 85.0^o. Both of these are within the error of the experimental[27] value of $86.0^o \pm 2^o$, which was extracted from data obtained at a $Re_D = 5000$. The drag coefficient for HRLES simulation is computed to be 1.5, which is significantly higher than the experimental[26] value of 0.99 ± 0.05, but is in line with the value of 1.65 obtained by similar LES simulations[26] computed also in two dimensions. The SST simulation resulted in a drag coefficient of 0.887.

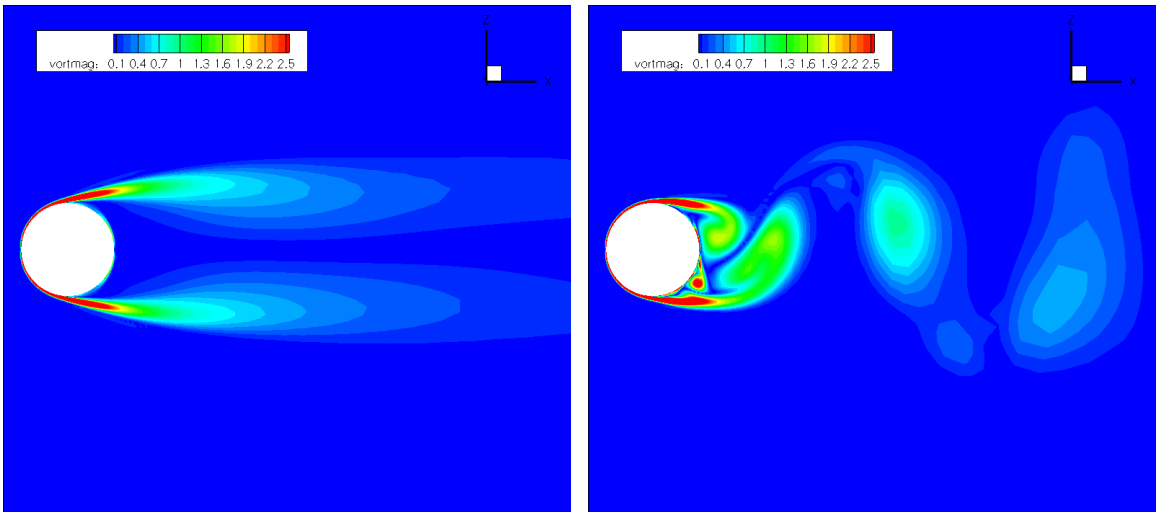

(a) $k-\omega SST$ (b) HRLES

Figure 4. Vorticity Magnitude about the Circular Cylinder

VI.B. NACA0015 Airfoil

The NACA0015 airfoil was run using the compressible option using the second-order spatial and first-order temporal algorithms. The flow was initialized by a short run using steady-state $k-\omega SST$ RANS model, prior to starting the time-accurate calculations. As observed in figure 8, the vorticity contours between the HRLES and RANS simulations are very different. The vorticity contours from this simulation are very similar to the ones observed by Sanchez-Rocha *et al.*[5] when the hybrid model was implemented in the LES code, as well as the KES simulations in OVERFLOW by Shelton *et al.*[6] At an angle of attack of 12^o, the HRLES shows the vortex shedding at the trailing edge, while none is observed in the RANS $k-\omega SST$ simulation. The separation location is approximately the same for both simulations. As the angle of attack is increased to 15^o, the trailing edge separation location has moved forward, and distinct vortex shedding just aft of this location is observed for the HRLES simulation. The RANS simulation still does not show trailing edge vortex shedding, and the difference in the prediction of the location of separation between HRLES and RANS are becoming obvious. Once an angle of attack of 18^o has been reached, the vortex shedding is now apparent for the RANS simulation, though it is significantly less than its HRLES counterpart, which shows both trailing and leading edge vortex shedding.

From an aeroacoustics perspective, the pressure field on and about the airfoil can be important in identifying the acoustic sources and noise magnitudes. Once again, at an angle of attack of 12^o, the pressure fields are very similar, but as the angle of attack is increased, significant differences in the instantaneous pressure field are noted. Further, the fluctuating pressures also are much different at the two higher angles of attack due to the complex vortex shedding and interaction of vortices above and in the wake of the airfoil.

VII. Conclusion

A hybrid Reynolds-Averaged Navier-Stokes (RANS) and Large Eddy Simulation (LES) turbulence method has been implemented and demonstrated in an unstructured legacy RANS computational fluid dynamics code. The hybrid method consists of a blending of the $k-\omega$ SST RANS model with a one equation LES model for the subgrid-scale turbulence kinetic energy (k^{sgs}). The model has been demonstrated for steady and unsteady flows for non-moving configurations. The next step is to add additional test cases, including three-dimensions and those where the configuration itself is unsteady, as is the case for a moving wing.

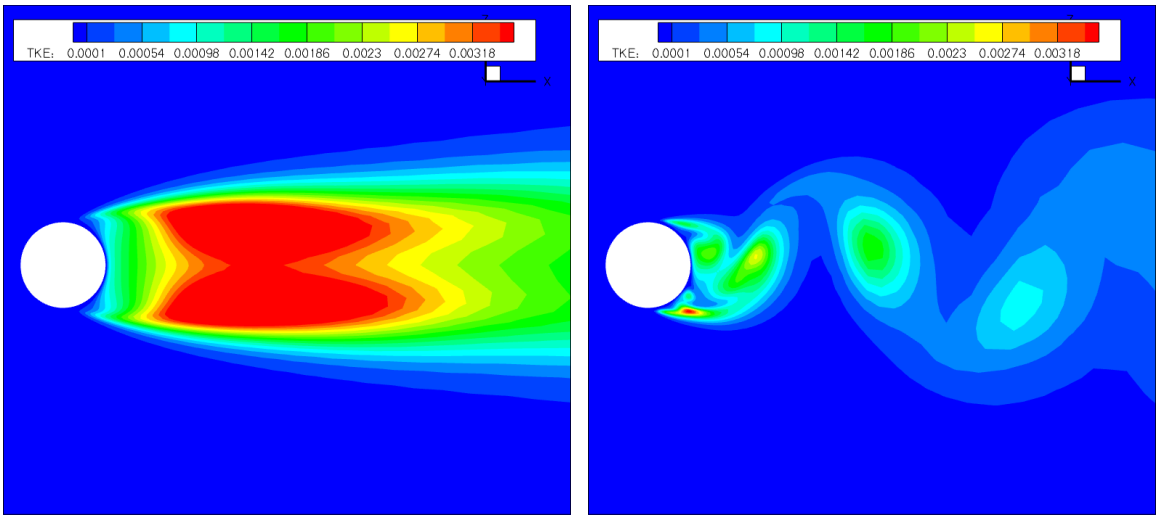

(a) $k - \omega SST$ (b) HRLES

Figure 5. Turbulent kinetic energy about the Circular Cylinder

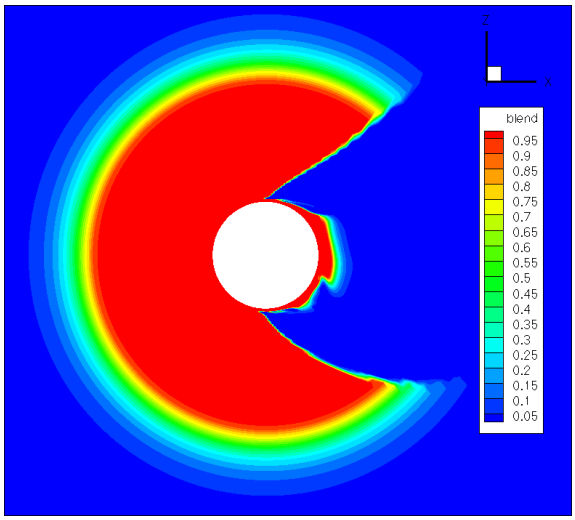

Figure 6. Blending function for the circular cylinder

Acknowledgments

This work was supported by the National Science Foundation, Project 0731034, "Advancing Wind Turbine Analysis and Design for Sustainable Energy". The authors would like to thank NSF and the NSF Program Officer is Dr. Trung Van Nguyen for their support in this endeavor. This research was supported in part by the National Science Foundation through TeraGrid[28] resources provided by TACC. The authors would like to thank Nicholas Burgess for his initial endeavors in this work, as well as the FUN3D Development Team for their aid and discussions.

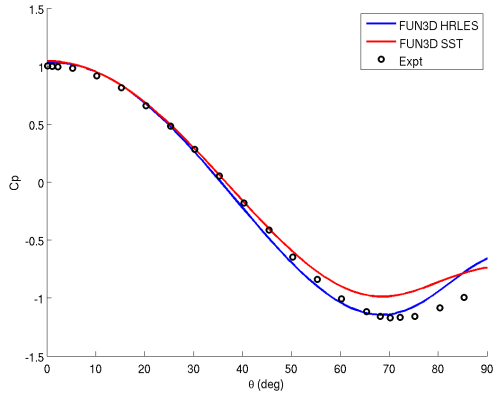

Figure 7. Instantaneous pressure coefficient for the circular cylinder

References

[1]D.C. Wilcox, *Turbulence Modeling for CFD*, CDW Industries, 2nd ed., 1998

[2]Smith, M. J., Wong, T.-C., Potsdam, M., Baeder, J. and Phanse, S., " Evaluation of CFD to Determine Two-Dimensional Airfoil Characteristics for Rotorcraft Applications." *Journal of the American Helicopter Society*, Vol. 51, No. 1, 2006.

[3]Szydlowski, J., and M. Costes, Simulation of flow around a NACA0015 airfoil for static and dynamic stall configurations using RANS and DES. Presented at the AHS International 4th Decennial Specialists' Conference on Aeromechanics, San Francisco, CA, January 21-23, 2004.

[4]Spalart, P.R., Jou, W.-H., Strelets, M., and Allmaras, S.R., "Comments on the Feasibility of LES for Wings, and on a Hybrid RANS/LES Approach," *Advances in DNS/LES*, C. Liu and Z.Liu, eds., Greyden Press, Columbus, OH, 1997.

[5]Sanchez-Rocha, M., Kirtas, M., Menon, S.,"Zonal Hybrid RANS-LES Method for Static and Oscillationg Airfoils and Wings", 4th AIAA Aerospace Sciences Meeting and Exhibit, Reno, Nevada, Jan. 9-12, 2006

[6]Shelton, A. B., Braman, K., Smith, M. J., Menon, S., "Improved Turbulence Modeling for Rotorcraft", American Helicopter Society 62nd Annual Forum, Phoenix, AZ, May 9-11,2006.

[7]Menter, F. R. *Improved Two-Equation k-ω Turbulence Models for Aerodynamic Flows*, NASA TM 103975, October 1992.

[8]Spalart, P. and Almaras, S., A One-Equation Turbulence Model For Aerodynamic Flows, AIAA Paper 92–0439, 1991.

[9]Fang, Y., and Menon, S., "A Two-Equation Subgrid Model for Large-Eddy Simulation of High Reynolds Number Flows," AIAA-06-0116, Reno, NV, Jan. 2006.

[10]Fang, Y. and Menon, S., "Kinetic-Eddy Simulation of Static and Dynamic Stall," AIAA -2006-3847, to be presented at the 24th AIAA Applied Aerodynamics Conference, San Francisco,CA, 5-8 June 2006.

[11]Bonhaus, D., *An Upwind Multigrid Method For Solving Viscous Flows On Unstructured Triangular Meshes*, M.S. Thesis, George Washington University, 1993.

[12]Smith, M. J., Wong, T.-C., Potsdam, M., Baeder, J. and Phanse, S., " Evaluation of CFD to Determine Two-Dimensional Airfoil Characteristics for Rotorcraft Applications." *Journal of the American Helicopter Society*, Vol. 51, No. 1, 2006.

[13]T. Renaud, D. M. O'Brien, Jr., M. J. Smith, and M. Potsdam, "Evaluation of Isolated Fuselage and Rotor-Fuselage Interaction Using CFD," *Journal of the American Helicopter Society*, Vol. 53, (1), 2008, pp. 3–17.

[14]Menon, S., and Kim, W.-W., "A New Dynamic One-Equation Subgrid Model for Large-Eddy Simulations," AIAA Paper No. 95–0356.

[15]Baurle, R. A., Tam, C. J., Edwards, J. R., and Hassan, H. A., "Hybrid Simulation Aproach for Cavity Flows: Blending, Algorithm, and Boundary Treatment Issues," *AIAA Journal*, Vol 41, No. 8, 2003, pp. 1463–1480.

[16]Speziale, C. G., "Turbulence Modeling for Time Dependent RANS and VLES: A review," *AIAA Journal*, Vol. 36, No. 2, 1998, pp. 173–184.

[17]Anderson, W., and Bonhaus, D., An Implicit Upwind Algorithm for Computing Turbulent Flows on Unstructured Grids, *Computers and Fluids*, Vol. 23, No. 1, 1994, pp. 1–21.

[18]Anderson, W., Rausch, R., and Bonhaus, D., Implicit/Multigrid Algorithms for Incompressible Turbulent Flows on Unstructured Grids, *Journal of Computational Physics*, Vol. 128, No. 2, 1996, pp. 391–408.

[19]OBrien, D. M., and Smith, M. J., "Analysis of Rotor-Fuselage Interactions Using Various Rotor Models," AIAA-2005-0468, January 2005.

[20]OBrien, D. M., *Analysis of Computational Modeling Techniques for Complete Rotorcraft Configurations*, PhD Thesis, Georgia Tech, May 2006.

[21]Lee-Rausch, E. M.,Frink, N. T., Mavriplis, D. J., Rausch, R. D. and Milholen, W. E., AIAA-2004-0554, "Transonic Drag Prediction on a DLR-F6 Transport Configuration Using Unstructured Grid Solvers," January 2004.

[22]Chorin, A., A Numerical Method for Solving Incompressible Viscous Flow Problems, *Journal of Computational Physics*, Vol. 2, No. 1, 1967, pp. 12–26.

[23]Roe, P., Approximate Riemann Solvers, Parameter Vectors, and Difference Schemes, *Journal of Computational Physics*, Vol. 43, Oct. 1981, pp. 357–371.

[24]Piziali, R., A., *2-D and 3-D Oscillating Wing Aerodynamics for a Range of Angles of Attack Including Stall*, NASA TM 4632, September 1994.

[25]Ong, L. and Wallace, J., The velocity eld of the turbulent very near wake of a circular cylinder, *Exp. Fluids*, Vol. 20, No. 441, 1996.

[26]Kravchenko, A. G., and Moin, P., "Numerical studies of ow over a circular cylinder at $Re_D = 3900$," *Physics of Fluids*, Vol. 12, No. 2, 2000, pp. 403–417.

[27]Son, J. and Hanratty, T. J., Velocity gradients at the wall for ow around a cylinder at Reynolds numbers 5×10^3 to 10^5, *J. Fluid Mech.*, Vol. 35, No. 353, 1969.

[28]Catlett, C. et al. "TeraGrid: Analysis of Organization, System Architecture, and Middleware Enabling New Types of Applications," HPC and Grids in Action, Ed. Lucio Grandinetti, IOS Press 'Advances in Parallel Computing' series, Amsterdam, 2007.

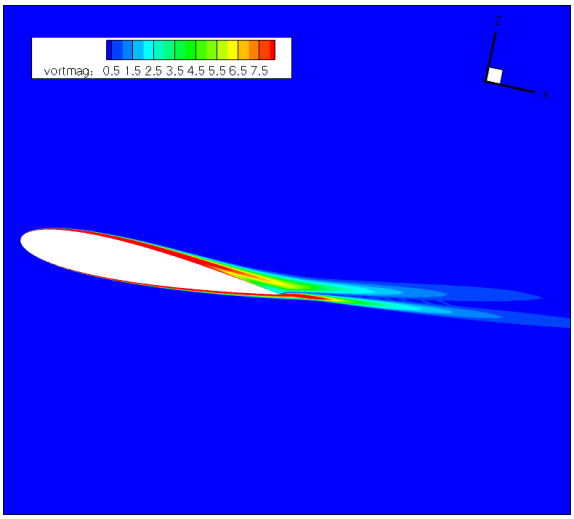

(a) RANS $\alpha = 12^o$

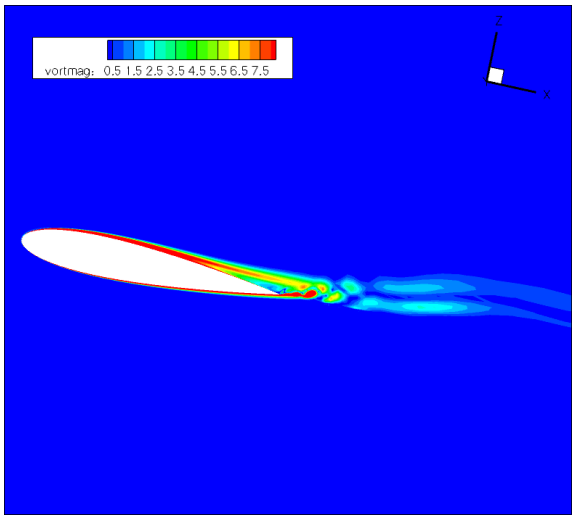

(b) HRLES $\alpha = 12^o$

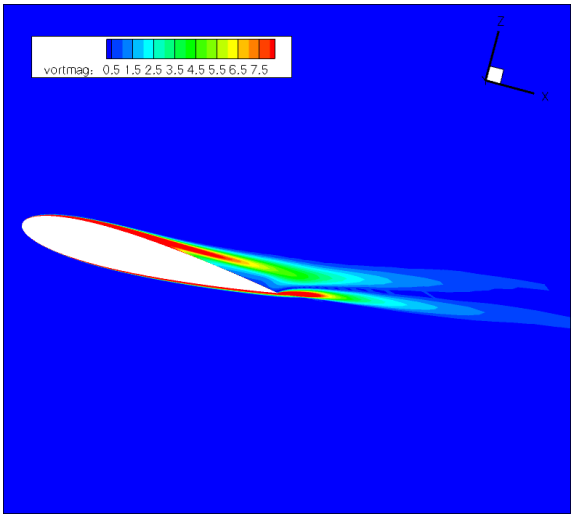

(c) RANS $\alpha = 15^o$

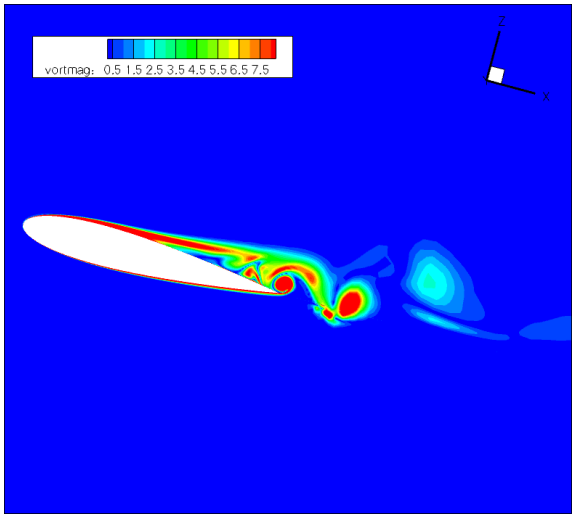

(d) HRLES $\alpha = 15^o$

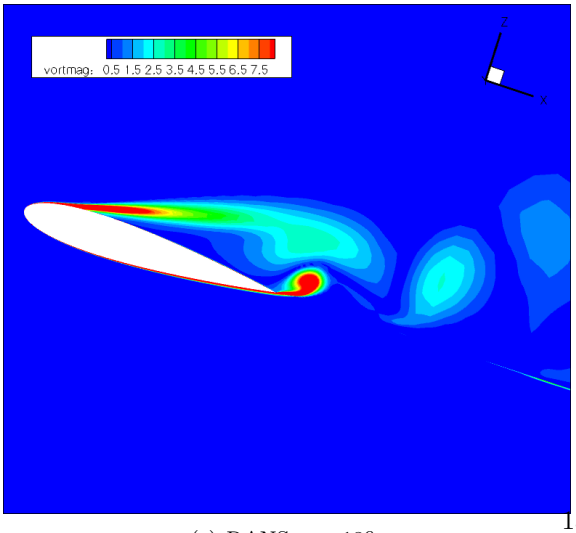

(e) RANS $\alpha = 18^o$

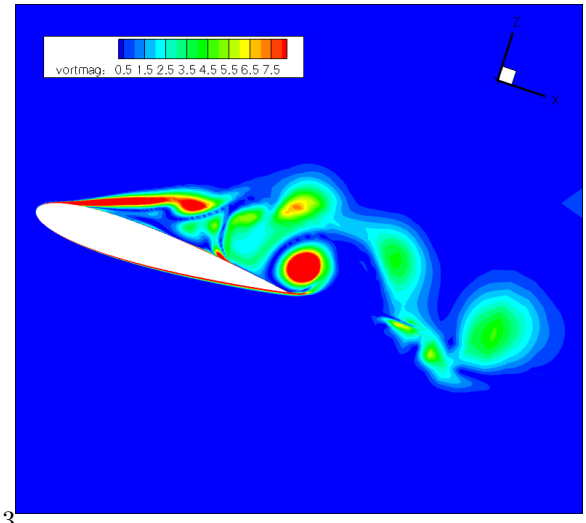

(f) HRLES $\alpha = 18^o$

Figure 8. Vorticity magnitude contours for the NACA0015 wing

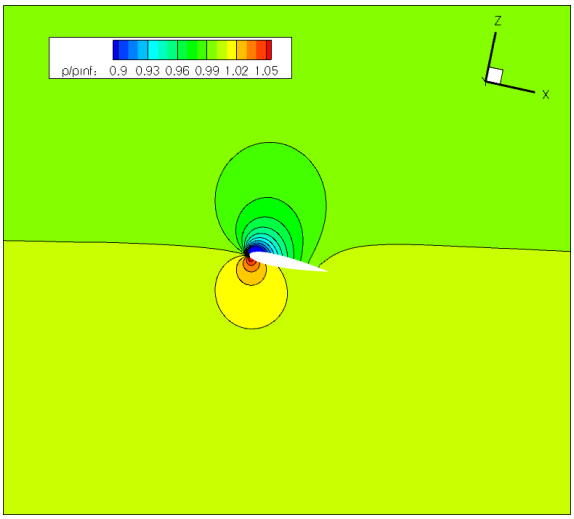

(a) RANS $\alpha = 12^o$

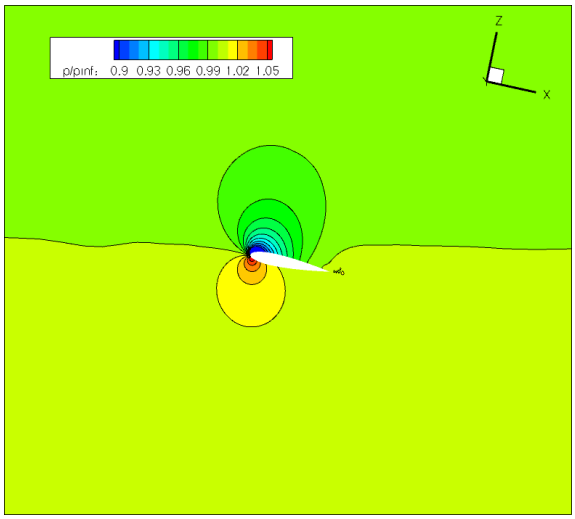

(b) HRLES $\alpha = 12^o$

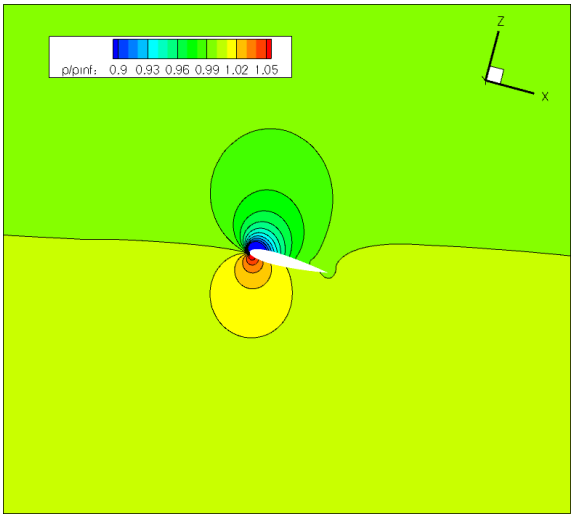

(c) RANS $\alpha = 15^o$

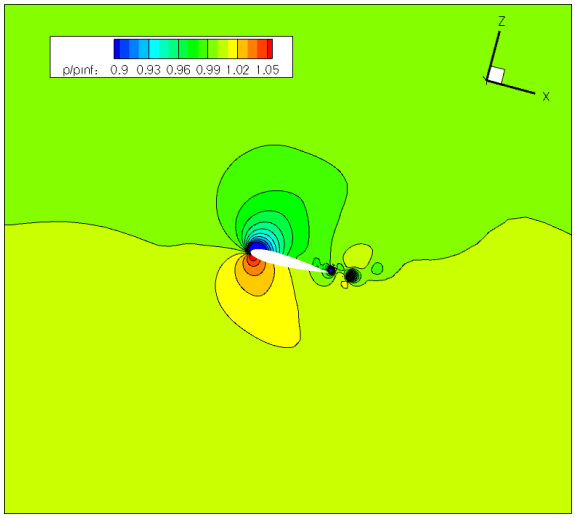

(d) HRLES $\alpha = 15^o$

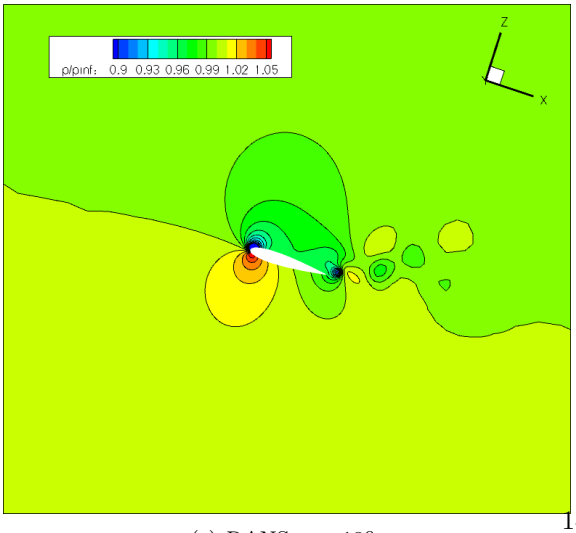

(e) RANS $\alpha = 18^o$

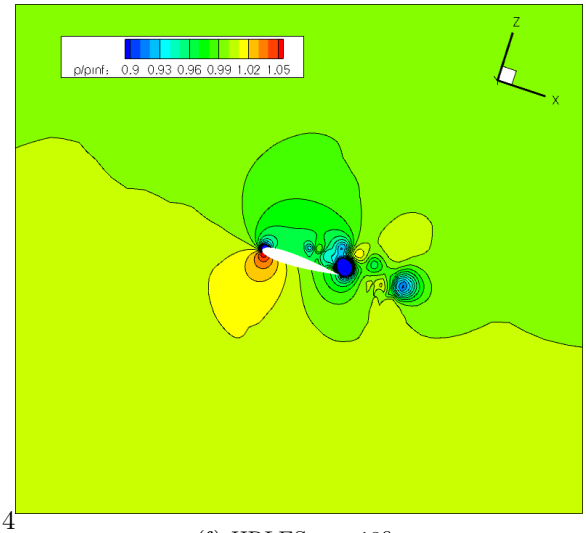

(f) HRLES $\alpha = 18^o$

Figure 9. Pressure contours for the NACA0015 wing